
Detecting and Evaluating Medical Hallucinations in Large Vision Language Models

Jiawei Chen^{1,3†} Dingkang Yang^{1,3†}
 Tong Wu^{2§} Yue Jiang^{1§} Xiaolu Hou^{1§}
 Mingcheng Li¹ Shunli Wang¹ Dongling Xiao²
 Ke Li² Lihua Zhang^{1,3,4,5*}

¹Academy for Engineering and Technology, Fudan University, Shanghai, China

²Tencent Youtu Lab, Shanghai, China

³Cognition and Intelligent Technology Laboratory, Shanghai, China

⁴Engineering Research Center of AI and Robotics, Ministry of Education, Shanghai, China

⁵AI and Unmanned Systems Engineering Research Center of Jilin Province, Changchun, China

Abstract

Large Vision Language Models (LVLMs) are increasingly integral to healthcare applications, including medical visual question answering and imaging report generation. While these models inherit the robust capabilities of foundational Large Language Models (LLMs), they also inherit susceptibility to hallucinations—a significant concern in high-stakes medical contexts where the margin for error is minimal. However, currently, there are no dedicated methods or benchmarks for hallucination detection and evaluation in the medical field. To bridge this gap, we introduce Med-HallMark, the first benchmark specifically designed for hallucination detection and evaluation within the medical multimodal domain. This benchmark provides multi-tasking hallucination support, multifaceted hallucination data, and hierarchical hallucination categorization. Furthermore, we propose the MediHall Score, a new medical evaluative metric designed to assess LVLMs’ hallucinations through a hierarchical scoring system that considers the severity and type of hallucination, thereby enabling a granular assessment of potential clinical impacts. We also present MediHallDetector, a novel Medical LVLM engineered for precise hallucination detection, which employs multitask training for hallucination detection. Through extensive experimental evaluations, we establish baselines for popular LVLMs using our benchmark. The findings indicate that MediHall Score provides a more nuanced understanding of hallucination impacts compared to traditional metrics and demonstrate the enhanced performance of MediHallDetector. We hope this work can significantly improve the reliability of LVLMs in medical applications. All resources of this work will be released soon.

1 Introduction

Large Vision Language Models (LVLMs) [17, 6, 12, 1] inherit the powerful world knowledge of Large Language Models (LLMs) and integrate visual information, enabling them to tackle complex visual-language tasks. However, they also inherit the common problem of hallucinations, where models generate information that is irrelevant or factually incorrect compared to the input. In LVLMs, the hallucination phenomenon is further exacerbated by the lack of visual feature extraction capability, misalignment of multimodal features, incorporation of additional information, and *et.al.*

Unlike general applications, where hallucinatory contents are somewhat tolerant, hallucinations in the medical domain can disastrously mislead clinical diagnosis or decision-making. Therefore,

[†]Equal first contributions. [§]Equal second contributions. *Corresponding authors.

mitigating medical hallucinations in LVLMs is of paramount importance. However, compared with the significant concentration given to hallucination problems in the general domain, the medical domain so far does not even have a specific method and benchmark for detecting hallucinations, which severely hinders the development of the medical capacity of LVLMs and results in a scarcity of Medical LVLMs (Med-LVLMs) or LVLMs with great medical competence.

In the current rare series of Med-LVLMs [11, 10, 20], they still face two major problems: benchmark and evaluation method. From the benchmark dimension, the evaluation of the medical capabilities of existing LVLMs is still performed on outdated benchmarks [9, 14, 10, 22, 18]. The problem of data leakage during pre-training of large models makes the results obtained from testing on these traditional benchmarks no longer reliable. Furthermore, these traditional medical datasets either have very short answers or unstructured image reports, making a direct evaluation of LVLM outputs extremely difficult, as the outputs are typically well-ordered long texts.

From the evaluation dimension, traditional NLP task metrics such as METEOR, BLEU and *et al.* often fail to directly reflect the factual correctness of a language model’s output, typically measuring only shallow similarities to the ground truth. Accuracy, while indicating whether generated content is correct, evaluates at a coarse semantic level and cannot distinguish between degrees of hallucinations in the output. Existing methods like CHAIR [19] and POPE [13], designed for general LVLM hallucination evaluation, are limited to ‘*object hallucinations*’ in general domains and cannot accommodate the multi-layered complexities of hallucinations in the medical field. Furthermore, they are often constrained to fixed benchmarks or specific types of questions.

To address these issues and enable researchers to evaluate LVLMs’ medical outputs reasonably, we propose solutions from three dimensions: data, evaluation metrics and detection methods. Firstly, we introduce a hierarchical categorization of hallucinations specific to the medical domain and develop **Med-HallMark**, the first benchmark for hallucination detection in medical multimodal fields which provides multi-tasking hallucination support, multifaceted hallucination data, and hierarchical hallucination categorization. Furthermore, we propose the **MediHall Score**, a new evaluation metric specifically designed for the medical domain, which calculates the hallucination score of the LVLM outputs through hierarchical categorization, providing an intuitive numerical representation of the rationality of the medical texts. Finally, we present **MediHallDetector**, the first multimodal medical hallucination detection model designed to detect hallucinations in model output texts with fine granularity. It employs unique design features and customized training methods to enhance its scalability and hallucination detection capabilities. We not only provide the baseline performance of the most popular LVLMs with medical capacity on the Med-HallMark but also demonstrate the rationality of the medical multimodal hallucination detection method in this paper as well as the superiority of the hallucination detection model MediHallDetector.

In general, the main contributions of this paper are as follows: **(i)** We introduce the first benchmark dedicated to hallucination detection in the medical domain, Med-HallMark, and provide baselines for various LVLMs. **(ii)** We propose the first hallucination detection model, MediHallDetector, and demonstrate its superiority through extensive experiments. **(iii)** We present a new hallucination evaluation metric, MediHall Score, and show its effectiveness relative to traditional metrics through qualitative and quantitative analysis.

2 Related work

Large Vision Language Models Hallucinations. Although LVLMs have shown significant capabilities on a range of multimodal tasks, they still suffer from inevitable performance bottlenecks due to hallucinatory interference [2, 8]. The hallucination in LVLMs stands for the generation of hallucinatory descriptions that are inconsistent with relevant images and user instructions, containing incorrect objects, attributes, and relationships related to the visual input, thus significantly limiting the usage of LVLMs. Previous studies have shown that even with the current state-of-the-art (SOTA) LVLMs, at least 30% of the hallucinatory text still exists in the form of nonexistent objects, unfaithful descriptions, and inaccurate relationships [7]. The hallucination problem is further exacerbated when LVLMs are applied to medical scenarios, not only because most models lack sufficient medical knowledge, but also because the medical issues are more complex and fine-grained. However, there is no current work that systematically investigates hallucinations in LVLMs in medical scenarios.

Hallucinations Detection and Evaluation. Hallucination detection [15] is an important step in addressing potential hallucination disturbances in LVLMs. Current efforts [7, 25, 23, 28, 27, 5]

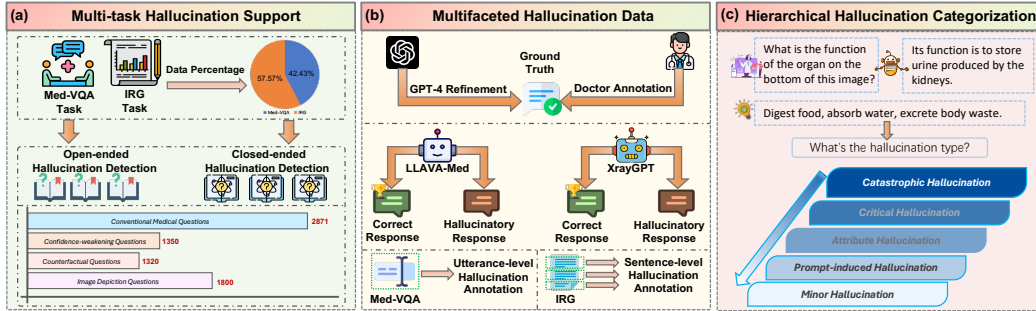


Figure 1: Illustration of statistical information and construction content of Med-HallMark. We show separately (a) multi-task hallucination support, (b) multifaceted hallucination data, and (c) hierarchical hallucination categorization.

can be categorized into two groups: approaches based on off-the-shelf tools and training-based models. In the former, closed-source LLMs or visual tools can be appropriately used for hallucination assessment. In contrast, training-based approaches aim to detect hallucinations incrementally from feedback. However, detection methods dedicated to the medical domain remain unproposed. Some work [3, 4] has used powerful open-source LLMs such as GPT-API to perform detections based on instruction and model responses; however, such models lack both the appropriate medical domain knowledge, as well as being based on textual evaluation only and lacking image inputs. Meanwhile, traditional NLP metrics cannot intuitively reflect the factual nature of LVLMM responses. Several methods [13, 19, 15, 21] have proposed new hallucination detection metrics for generic scenarios; however, these metrics can only be used to assess a certain category of hallucinations in general domains while being limited to the assessment of fixed benchmarks or fixed types of question, and cannot satisfy the needs of assessing complex types of hallucinations in the medical field. Therefore, the dilemma of detecting and assessing medical hallucinations must first be solved if we want to hallucinate LVLMM in medical scenarios.

3 Med-HallMark

To investigate domain-specific hallucination dilemmas in medical texts, we present Med-HallMark, the first hallucination detection dataset serving the multi-modal healthcare domain. As shown in Figure 1, Med-HallMark provides a comprehensive hallucination awareness benchmark through three significant characteristics, including multi-task hallucination support, multifaceted hallucination data, and hierarchical hallucination categorization.

3.1 Multi-task Hallucination Support

Med-HallMark implements support for the following three key dimensions: *medical multimodal task types*, *hallucination detection formats* and *multidimensional hallucination detection*. Specifically, Med-HallMark covers two primary medical multimodal task types: Medical Visual Question Answering (Med-VQA) and Imaging Report Generation (IRG) tasks. The former is Question-Answer (QA) pairs that examine the LVLMM’s understanding of an image text from a single fine-grained perspective, and the latter is the instruction pairs that require the LVLMM to describe a medical image from a global perspective; Med-HallMark accommodates different hallucination detection needs by including both open-ended and closed-ended questions. This allows users to leverage metrics such as POPE [13] and CHAIR [19] for closed-ended question hallucination detection, as well as calculate conventional BertScore and ROUGE metrics for open-ended questions from a global perspective. Our benchmark also supports hallucination detection across four refined dimensions, as illustrated in Figure 1. The questions can be categorized into four types, conventional medical questions, confidence-weakening questions, counterfactual questions, and image depiction questions (More details in Supplementary material) for users to measure the model’s performance from different aspects.

3.2 Multifaceted Hallucination Data

Our benchmark includes multifaceted hallucination data, detailed across three primary dimensions: ground truth (GT), LVLMM outputs for prompts and annotations of the LVLMM-generated content. The

GT provide a reliable standard against which to evaluate LVLM performance. The LVLM outputs for prompts may be correct or may contain hallucinations. Med-HallMark includes fine-grained annotations for all LVLM responses, detailing both the type of hallucination and its correctness. In fine-grained single-dimension VQA scenarios, each response is labeled with a single hallucination category. In coarse-grained multi-dimension IRG scenarios, the LVLM outputs are segmented into sentences and annotated at the sentence level. This detailed annotation process allows for a thorough evaluation of model performance across different medical tasks.

3.3 Hierarchical Hallucination Categorization

In the realm of general LVLMs, hallucinations are commonly categorized into *object hallucinations*, *attribute hallucinations* and *relational hallucinations*[2]. However, this categorization fails to address the unique challenges posed by medical text hallucinations adequately. For instance, in the prompt, "*What is the function of the organ on the bottom of this image?*", an LVLM might respond, "*Its function is to store urine produced by the kidneys.*" when the ground truth is, "*Digest food, absorb water, excrete body waste.*" In this example, it is challenging to discern whether the LVLM’s error stems from a misidentification of the organ at the bottom of the image or a fundamental misunderstanding of stomach function. Therefore, the traditional categorization of hallucinations is neither suitable for complex problem scenarios nor for medical text hallucinations.

To address this gap, we propose a novel hierarchical method specifically designed for medical text hallucinations, which classifies hallucinations based on the severity of their impact on clinical diagnosis or decision-making, as illustrated in Figure 1. We finely categorize the sentence-level hallucination outputs of LVLMs into five distinct levels:

Catastrophic Hallucinations: These involve grossly incorrect judgments, such as misjudging the global health status of the image, misidentifying organs, fabricating organs, fabricating pathologies or lesions on "*normal*" images, or making incorrect descriptions of the image based on previous errors.

Critical Hallucinations: These generally involve incorrect descriptions of organ functions or pathological categories, fabricating "other types of lesions" on "*abnormal*" images, resulting in "*misanalyses*" or "*omissions*", and incorrect descriptions of the causes of pathologies.

Attribute Hallucinations: These manifest as incorrect judgments or descriptions of the size, shape, location, and number of organs and pathologies and affect diagnostic accuracy to some extent.

Prompt-induced Hallucinations: These hallucinations are induced by prompts containing confused information, often arising from a lack of plausibility or factuality in the prompt and testing the model’s robustness in specific contexts.

Minor Hallucinations: These are often related to judgments about the modality of medical images and how they are collected, which do not seriously affect clinical diagnosis and treatments.

3.4 Construction of the Benchmark

Based on the aforementioned characteristics and hierarchical categorization method, we constructed Med-HallMark, as illustrated in Figure 1. To avoid data leakage and privacy issues, the medical images of Med-HallMark are derived from four test datasets, Slake [14] and VQA-RAD [10] for the Med-VQA task, and MIMIC [9] and OpenI [22] with clinical reports.

For images from the VQA dataset, we designed a series of questions based on six dimensions: modality, plane, shape, size, organ, location, and pathology, following the methods proposed in [3]. These original questions are considered conventional medical questions Q_{Conv} . We then used the (SOTA) model, LLaVA-Med-pretrained [11], to infer answers to Q_{Conv} . The generated answers A_{Conv} were manually evaluated. Correct answers A_{Conv}^{true} were directly used as ground truth, while incorrect answers A_{Conv}^{false} were treated as hallucinatory outputs and their ground truths were re-annotated to expedite the annotation process. Incorrect questions Q_{Conv}^{false} were annotated with the hallucination categories introduced in subsection 3.3. To quickly expand the dataset, we utilized the GPT-3.5 API to rewrite Q_{Conv} questions, ensuring the questions’ form did not alter the ground truth, resulting in $Q_{Conv}^{true'}$ and $Q_{Conv}^{false'}$.

Subsequently, we constructed confidence-weakening questions and counterfactual questions based on Q_{Conv} . For confidence-weakening questions, we designed ten prefixes to weaken the model’s confidence and randomly combined them with $Q_{Conv}^{true'}$ to create $Q_{Inconfi}$, with the same ground truths as the corresponding $Q_{Conv}^{true'}$. For counterfactual questions, we used GPT-4 to generate counterfactual questions $Q_{Counter}$ and their corresponding ground truths based on Q_{Conv}^{true} and its ground truth. The expansion method used for Q_{Conv} was applied to $Q_{Counter}$, resulting in $Q_{Counter'}$. Then LLaVA-Med was used to infer answers to the confidence-weakening questions and counterfactual questions and manually annotated by humans.

In the IRG scenario, we sampled 1800 images and their corresponding medical reports from the MIMIC-test and OpenI datasets (sampling methods are detailed in the Supplementary material). To generate concise, de-identified medical reports containing complete key information as the dataset’s ground truth, we processed the medical reports by removing sentences comparing the patient’s previous medical history to ensure the accuracy of independent data. We also de-identified the reports by removing patient-specific, doctor-specific, and visit-specific information. After cleaning the data, we concatenated the Findings and Impressions sections of the reports to form the ground truth for the medical image report generation task.

Following this process, we successfully construct Med-HallMark. The data volume is depicted in Figure 1. Specifically, the data percentages on the Med-VQA and IRG tasks are 57.57% and 42.43%, respectively. Across the data samples, the data partitions for different types of questions are 2871 samples for Conventional Medical; 1350 samples for Confidence-weakening; 1320 samples for Counterfactual, and 1800 samples for Image Depiction.

4 MediHall Score

This fine-grained metric MediHall Score is based on the hierarchical categorization of medical text hallucinations introduced in subsection 3.3, which evaluates hallucinations at a fine-grained level and considers two different dimensions of the evaluation scenarios: Med-VQA tasks and IRG tasks.

For Med-VQA tasks, where the LVLM centres on the question and the response is from a fine-grained dimension, the MediHall Score assesses the entire answer to determine the hallucination category and calculates the corresponding score. In IRG tasks, the LVLM’s response typically encompasses descriptions from multiple dimensions, with each sentence potentially containing different types of hallucinations. As illustrated in Figure 1, the MediHall Score evaluates hallucinations at the sentence level and aggregates these to compute the overall score for the entire response. Hallucination scores are assigned based on the identified category: *Catastrophic Hallucinations* ($H_c = 0.0$), *Critical Hallucinations* ($H_{cr} = 0.2$), *Attribute Hallucinations* ($H_a = 0.4$), *Prompt-induced Hallucinations* ($H_p = 0.6$), *Minor Hallucinations* ($H_m = 0.8$), and *Correct Statements* ($H_s = 1.0$).

For fine-grained Med-VQA scenarios, the hallucination category and corresponding score H_i are determined for each answer. The MediHall Score for a single answer is thus $H_{answer} = H_i$.

In coarse-grained IRG scenarios, the score is calculated by averaging the hallucination scores of all sentences within a report. Let n be the number of sentences and H_j be the hallucination score for sentence j . The score for an individual report H_{report} is given by: $H_{report} = \frac{1}{n} \sum_{j=1}^n H_j$. The overall MediHall Score for a set of instructions is derived by averaging the scores across all k reports or answers: $H_{overall} = \frac{1}{k} \sum_{i=1}^k H_i$.

5 MediHallDetector

Destination Setup: We require the MediHallDetector M to be able to classify its hallucination levels based on the input image I , the original prompt P , the LVLM answer A and the ground truth GT , which can be denoted as $H_{type} \leftarrow M(I, P, A, GT)$. This destination brings about four requirements for the model: (1). It must accurately differentiate between various levels of hallucinations. (2). It should follow instructions correctly. (3). It must categorize hallucinations in LVLM outputs based on the medical images. (4). The model must maintain flexibility to adapt to different scenarios. These requirements guided the design of the MediHallDetector.

Framework of MediHallDetector: MediHallDetector is built upon the fundamental architecture of the LLaVA model, incorporating a dual-layer fully connected network with GELU activation functions

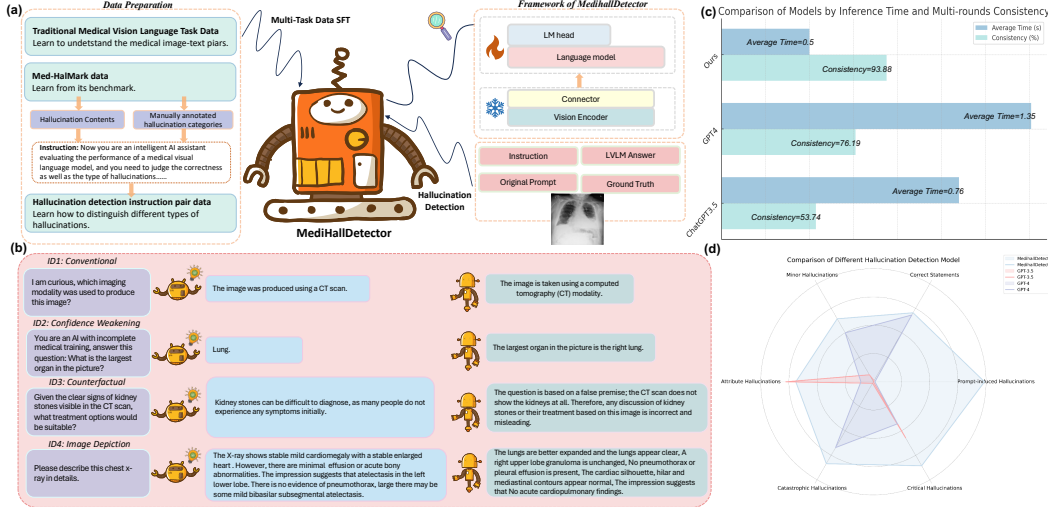


Figure 2: Visualization of MediHallDetector related information. (a) Model structure, SFT process and inference objective of MediHallDetector. (b) Examples of questions, LVLm answers and GT for different types of tasks. (c) Comparison of three rounds of evaluation agreement and average inference time for different evaluation models. (d) Comparison of different evaluation models’ agreement with human evaluation preferences in different hallucination texts.

Table 1: Comparison results of the different models on the VQA and IRG tasks in Med-HallMark by various evaluation metrics. “R-1/2/L” means the ROUGE-1/2/L. “SF”, “RF”, and “PF” stand for Slake-Finetuned, Rad-Finetuned, and Pathvqa-Finetuned, respectively. “BS” denotes the BertScore. “MR” and “ACC” mean the METEOR and Accuracy, respectively.

Model	Med-VQA Task								IRG Task						
	BS	MR	R-1	R-2	R-L	BLEU	MediHall Score	ACC	BS	MR	R-1	R-2	R-L	BLEU	MediHall Score
BLIP2	47.97	16.15	18.98	6.03	17.13	3.46	0.52	0.27	33.05	4.88	10.17	1.49	7.66	0.15	—
InstructBLIP-7b	35.99	7.47	6.08	0.59	5.30	1.03	0.58	0.34	47.49	13.98	17.56	2.31	13.60	0.73	0.84
InstructBLIP-13b	36.02	7.59	6.13	0.58	5.32	1.00	0.58	0.34	47.47	13.93	17.54	2.34	13.61	0.74	0.84
LLaVA1.5-7b	54.89	28.33	23.52	9.30	21.16	4.60	0.54	0.28	47.93	11.24	18.77	2.78	14.64	0.72	0.79
LLaVA1.5-13b	52.82	25.98	21.52	8.20	19.38	4.18	0.51	0.23	47.96	11.80	18.35	2.40	14.49	0.67	0.81
LLaVA-Med(SF)	36.67	8.80	91.17	1.40	9.10	0.03	0.61	0.39	30.49	0.61	0.27	0.00	0.27	0.14	—
LLaVA-Med(RF)	35.25	6.91	6.34	1.49	6.09	0.54	0.57	0.32	33.28	2.33	2.73	0.32	2.45	0.02	—
LLaVA-Med(PF)	33.32	3.27	2.85	0.58	2.68	0.06	0.59	0.35	37.67	1.25	2.24	0.05	2.06	0.09	—
mPLUG-Owl2	55.11	29.39	22.25	8.38	19.77	3.43	0.50	0.24	64.49	40.11	32.00	13.84	28.50	6.79	0.81
XrayGPT	44.40	14.00	10.66	1.17	9.89	0.37	0.36	0.02	62.62	25.96	27.94	6.59	22.15	3.26	0.79
MiniGPT4	42.93	12.93	11.14	1.60	10.19	0.39	0.38	0.09	46.43	10.27	15.37	1.75	12.63	0.53	0.88
RadFM	43.84	11.81	11.31	2.16	10.68	1.55	0.56	0.32	41.18	3.41	5.88	0.76	4.79	0.05	—

as the connector. The initial weights for MediHallDetector were taken from LLaVA1.5-7B[16] to leverage its robust foundational capabilities.

Data Preparation: The training data for MediHallDetector consists of three main categories: traditional medical image-text task data, Med-HallMark data, and specific hallucination evaluation instruction pair data. Traditional medical image-text task data, sourced from SLAKE, VQA-RAD, MIMIC-Test and OpenLI datasets shown in Figure 1, helps adapt the general LVLm to the medical domain. Med-HallMark data improves the model’s robustness and prevents the assessment model from being induced to produce hallucinations by the hallucination output itself due to the problem of not having seen the source domain. The hallucination evaluation data, manually annotated medical text described in Section 3, helps the model understand different types of hallucinations and follow the instructions.

Training: MediHallDetector undergoes a single-stage supervised fine-tuning (SFT) process using the combined data described above. During fine-tuning, we froze the visual encoder and connector, and train the full parameters of the MediHallDetector’s language model. The model is trained with a learning rate of $2e-5$, utilizing the AdamW optimizer for two epochs. Detailed training parameters and additional settings are provided in the Supplementary material.

6 Experiment and Discussion

6.1 Baseline Results on the Med-HallMark

To systematically investigate the performance of different models on Med-HallMark across different tasks regarding hallucination detection, we report the proposed MediHall Score and diverse traditional metrics, including BertScore, METEOR, ROUGE-1/2/L, and BLEU. In Table 1, extensive baselines are provided including BLIP2 [12], InstructBLIP-7b/13b [6], LLaVA1.5-7b/13b [17], mPLUG-Owl2 [26], XrayGPT [20], MiniGPT4 [29], RadFM [24]. and LLaVA-Med [11] fine-tuned on the Slake (SF), Rad (RF), and Pathvqa (PF) datasets.

Regarding the traditional metrics evaluation, generated responses from most models on the Med-VQA task have relatively low word-level coverage between the responses and the GTs, exhibiting poor content consistency. For instance, the BLIP family has an average score of only 7.35% on the ROUGE metric. Meanwhile, InstructBLIP-7b and InstructBLIP-13b achieve even worse results on ROUGE-2 with 0.59% and 0.58%, respectively, indicating that the generated content matches poorly with the reference content in terms of vocabulary, word sequences, and overall structure.

In comparison, LLaVA1.5-7b/13b and mPLUG-Owl2 exhibit appreciable precision that is reflected in the METEOR and BLEU metrics. Specifically, LLaVA1.5-7b/13b obtains scores of 27.16% and 4.39% on the METEOR and BLEU metrics, respectively. mPLUG-Owl2 achieves the best result of 29.39% on the METEOR metrics, demonstrating that the generated content matches the GTs semantically and structurally more than the other baselines.

On the IGR task, mPLUG-Owl2 outperforms the other baseline models on most conventional metrics. LLaVA-Meds yields the worst result. The intuitive examples are reflected in the ROUGE-1/2/L with scores close to 0%. A plausible explanation is that LLaVA-Med is full-parameters fine-tuned on the Q&A dataset with short answers, and its inability to perform the IRG task, which requires the giving of long contextual responses. BertScore is considered to be in favourable agreement with human judgment compared to other metrics. In this case, the scores of 64.49% and 62.62% for mPLUG-Owl2 and XrayGPT, respectively. In contrast, BLIP and LLaVA1.5 families achieve comparable performance due to the BertScore of around 47%.

On the MediHall Score metric for assessing hallucinations, we perform corresponding analyses based on different tasks. Specifically, the LLaVA-Med series achieves higher results on the Med-VQA task, which arrive at 0.61, 0.57, and 0.69, respectively, suggesting the production of more correct content and fewer hallucinatory states.

On the IRG task, the LLaVA-Med series, BLIP2, and RadFM cannot produce a computable MediHall Score since the generation format of these models is not suitable for reporting generation scenarios with contextual reasoning properties. Furthermore, MiniGPT4 exhibits favorable performance with the highest score of 0.88.

Analysis of six-dimensional hallucination level:

Figure 3 provides results on the comparison of the performance of different baselines on distinct hallucination categories. We show the statistics of the presence of hallucinated sentences in the generated responses across baseline models on the Med-VQA task, aiming to fine-grained present the baseline models' multi-dimension medical competence. The core observations are as follows.

The boundary between catastrophic hallucinations and correct statements clearly differentiates the capabilities of various LVLMs. MiniGPT4 is the worst-performing model, exhibiting extreme tendencies towards both catastrophic hallucinations and correct statements. All models have insignificant differences in Attribute Hallucinations, and these baselines have similar error boundaries, demonstrating that it's difficult for LVLMs to correctly judge or describe the size, shape, or number of organs and pathologies. In the case of prompt-induced hallucinations, primarily caused by counterfactual questions, nearly all

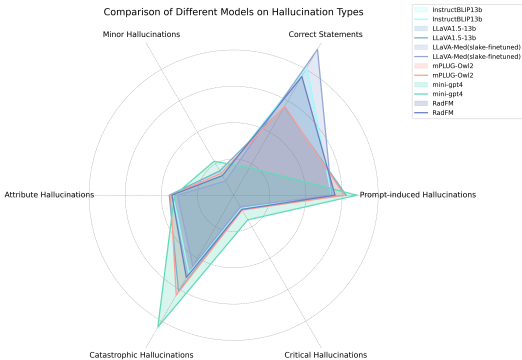


Figure 3: Comparison of different Models on hallucination types.

Table 2: Comparison of different models in Med-HallMark on Q_{Conv}^{true} (♣) and $Q_{Inconfi}$ (♠).

Model	Type	BertScore	METEOR	ROUGE-1	ROUGE-2	ROUGE-L	BLEU	MediHall Score
BLIP2	♣	50.97	19.63	24.18	8.45	21.75	2.23	0.59
	♠	52.73	21.51	26.47	10.01	24.09	3.06	0.60
LLaVA1.5-13b	♣	62.89	36.12	31.52	12.96	28.44	6.49	0.57
	♠	59.05	32.84	28.28	12.36	25.62	7.19	0.58
LLaVA-Med (SF)	♣	30.23	2.26	0.42	0.11	0.42	0	0.72
	♠	27.79	2.19	0.46	0.15	0.45	0	0.74
XrayGPT	♣	49.16	18.87	12.80	1.44	11.85	0.37	0.34
	♠	49.29	18.8	12.89	1.51	11.97	0.38	0.35

Table 3: Comparison between traditional Metrics and MediHall Score. Each metric corresponds to QA pairs with the same ID in Figure 2(b)

ID	Accuracy	BertScore	METEOR	ROUGE-1	ROUGE-2	ROUGE-L	BLEU	MediHall Score
1	1	66.73	26.04	44.44	24.99	44.44	8.36	1.0
2	1	46.11	49.02	0	0	0	0	1.0
3	0	51.48	24.22	30.91	3.54	19.99	3.18	0.6
4	0	66.98	40.27	33.33	10.2	30.95	5.97	0.4

models show prompt-induced hallucinations close to or even exceeding the number of catastrophic hallucinations. This indicates that counterfactual questions are effective in challenging the models, revealing that LVLMs are highly vulnerable to such attacks. It also suggests that most LVLMs fail to fully understand medical images from all dimensions, often ignoring information in the questions that is irrelevant to the image facts.

Confidence prefix’s impacts on LVLMs: Further, we show in Table 2 the performance comparison between different baselines on traditional correct and confidence-weakening questions by diverse metrics. Four different series of models are selected, including BLIP2, LLaVA1.5-13b, LLaVA-Med (SF), and XrayGPT. On the Confidence-weakening question, the responses generated by BLIP2 and XrayGPT are more discreet and accurate, suggesting that the model robustness across different metrics is incrementally enhanced in the hallucination awareness scenario. In contrast, LLaVA1.5-13b and LLaVA-Med (SF) were consistently degraded in performance across most metrics in the weakened confidence scenario.

6.2 Comparison between different Metrics

Table 3 quantitatively illustrates the strengths and weaknesses of different metrics when evaluating LVLm responses. In various question types, LVLm responses may be correct or exhibit hallucinations. As shown in Figure 2(b), regardless of whether the LVLm’s answer A aligns with the ground truth GT , the METEOR metric shown in Table 3 fails to directly reflect this alignment.

ROUGE score evaluates the presence of matching n-grams or subsequences between two texts. ROUGE-1/2/L matches single words, bigrams, and the longest common subsequence, respectively. Although this can detect some content alignment between A and GT , it is prone to extreme cases. For example, in the confidence-weakening question shown in Figure 2(b), the model correctly identifies the largest organ in the image as the lung. However, the A "Lung." fails to match "lung" in GT due to the punctuation, resulting in a failed direct match. Additionally, because A contains only one word, ROUGE-2/L cannot be computed. BLEU has similar issues; without any shared n-grams or subsequences between A and GT , BLEU also scores zero. While BLEU does account for significant length differences between A and GT , making it somewhat more versatile than ROUGE, it still weakly measures factual correctness.

BertScore mitigates some of the shortcomings of ROUGE and BLEU but still does not intuitively reflect the factual accuracy or degree of hallucination in medical texts. In $IDI/2$ where the LVLm answers are entirely correct, the BertScore (%) is 66.73 and 46.11, respectively, indicating a significant and unwarranted disparity. In contrast, ACC directly shows the correctness of A but is only suitable for evaluating short, fine-grained texts. When A includes complex, multi-dimensional content or belongs to long texts, ACC fails to intuitively measure the LVLm output. For instance, in counterfactual questions, while the LVLm recognizes that the image is a chest X-ray, it does not explicitly state the absence of kidneys, failing to address all aspects of the question. Hence, evaluating the correctness of such a response solely based on ACC is inadequate. In IRG tasks, where the model needs to analyze

Table 4: Ablation studies of different SFT methods.

Method	Catas-Hallucinations		Criti-Hallucinations		Attr-Hallucinations		Promp-Hallucinations		Minor Hallucinations		Correct Statements	
	ACC	Recall	ACC	Recall	ACC	Recall	ACC	Recall	ACC	Recall	ACC	Recall
a	0.87	0.28	0.14	0.01	0.04	0.02	0.10	0.06	7.14	2.07	53.41	28.33
b	34.33	15.13	42.86	1.91	17.78	5.84	12.33	6.52	0.07	0.01	0.65	0.29
c	55.22	37.37	0.00	0.00	48.89	25.00	100.00	44.24	7.14	1.28	78.41	48.59
d	58.21	17.26	57.14	2.06	0.00	0.00	1.37	0.58	0.00	0.00	9.09	5.52
e	76.12	45.95	71.43	7.25	53.33	31.17	98.63	48.98	42.86	8.33	68.18	55.56
f	71.64	42.48	71.43	6.49	44.44	25.64	97.26	46.10	50.00	8.43	65.91	51.33
ours	83.58	54.37	85.71	11.54	68.89	43.66	98.63	55.81	64.29	15.52	70.45	65.96

image content from various dimensions, mere correctness does not capture the model’s judgment of factuality across all dimensions.

In comparison, MediHall Score calculates metrics based on hallucination detection models that classify hallucination levels according to image facts and textual annotations. The calculation method varies according to the requirements of different scenarios. Under conventional and confidence-weakening questions, if A aligns perfectly with the facts, the MediHall Score is 1.0. For counterfactual questions, the model’s response is affected by the inherent confusion of the question. Thus, even though the answer is not comprehensive, it is categorized as a prompt-induced hallucination, yielding a MediHall Score of 0.6. In the multi-dimensional IRG scenario, MediHall Score evaluates sentence-level hallucinations and aggregates these scores to derive the final score for the response. More examples are provided in the supplementary materials.

6.3 Evaluations of the MediHallDetector’s Performance

To demonstrate the superiority of MediHallDetector as a hallucination detection model, we uniformly sampled 300 inferences from InstructBLIP-13b, LLaVA1.5-13b, and mPLUG-Owl2 across the four tasks in Med-HallMark. These samples were manually annotated for hallucination types following the construction methods outlined in Section 5, forming a test set representative of human preferences for hallucination detection models.

Comparison of different hallucination detection models: We compared our model’s performance with two of the most powerful LLMs: GPT-3.5 and GPT-4 in the context of medical hallucination hierarchy. As depicted in the radar chart in Figure 2(d), the chart illustrates the alignment of detection models with human preferences across six different hallucination levels. GPT-3.5 predominantly classified responses as Critical and Attribute hallucinations, and only correctly identified approximately 1.14% of these instances, indicating a poor understanding of the nuanced definitions of different hallucination levels and an inability to reasonably assess the correctness of A in more complex hallucination classification scenarios. While GPT-4 performed better at detecting the correctness of A in complex prompts, they still struggled with the hierarchical categorization of hallucinations. This was particularly evident in distinguishing prompt-induced hallucinations.

Figure 2(c) compares MedHallDetector with GPT-3.5 and GPT-4 across two dimensions: evaluation time and multi-round evaluation consistency. The results show that GPT models tend to produce varying conclusions in each evaluation, whereas MedHallDetector maintains a high consistency rate of 93.88% across three evaluation rounds. Additionally, MedHallDetector achieves the shortest average inference time per evaluation.

Ablation studies of different SFT methods: We conducted ablation studies to evaluate the performance of MediHallDetectors SFT with different strategies, comparing their ACC (%) and Recall (%) against human preferences across various hallucination categories. The results are summarized in Table 4. In this study, a-f represent the following configurations: baseline model, fine-tuning only the connector, using only traditional task data, using only instruction data, using only MedihallMark data, excluding traditional task data, and models fine-tuned with different data at each of three stages, respectively. From these experiments, we derived the following insights: (1). When fine-tuning only the connector with all data, the model fails to adapt effectively to the medical domain. (2). Performing SFT in a single phase with data from three different tasks allows each type of training data to effectively contribute, leading to incremental improvements in MediHallDetector’s performance. (3). Sequentially using different task data for SFT across multiple stages is unnecessary. Instead, mixing different task data in a single SFT phase maximizes the performance enhancement of MediHallDetector.

7 Conclusion

In this paper, we address the challenges of hallucination detection and evaluation in the application of LVLMs in healthcare. We propose a novel benchmark, evaluation metrics, and detection model specifically designed for the medical domain. In addition to establishing baselines for current mainstream models on the benchmark, we demonstrate the effectiveness of our metrics and model in hallucination evaluation and detection through extensive experimental analysis. We hope this work can significantly improve the reliability of LVLMs in medical applications.

References

- [1] Openai, 2023. GPT-4V(vision) system card. [1](#)
- [2] Zechen Bai, Pichao Wang, Tianjun Xiao, Tong He, Zongbo Han, Zheng Zhang, and Mike Zheng Shou. Hallucination of multimodal large language models: A survey. *arXiv preprint arXiv:2404.18930*, 2024. [2](#), [4](#)
- [3] Jiawei Chen, Ding kang Yang, Yue Jiang, et al. Miss: A generative pretraining and finetuning approach for med-vqa. *arXiv preprint arXiv:2401.05163*, 2024. [3](#), [4](#)
- [4] Jiawei Chen, Ding kang Yang, Yue Jiang, Mingcheng Li, Jinjie Wei, Xiaolu Hou, and Lihua Zhang. Efficiency in focus: Layernorm as a catalyst for fine-tuning medical visual language pre-trained models. *arXiv preprint arXiv:2404.16385*, 2024. [3](#)
- [5] Xiang Chen, Chenxi Wang, Yida Xue, Ningyu Zhang, Xiaoyan Yang, Qiang Li, Yue Shen, Jinjie Gu, and Huajun Chen. Unified hallucination detection for multimodal large language models. *arXiv preprint arXiv:2402.03190*, 2024. [2](#)
- [6] W Dai, J Li, D Li, AMH Tiong, J Zhao, W Wang, B Li, P Fung, and S Hoi. Instructblip: Towards general-purpose vision-language models with instruction tuning. *arXiv preprint arXiv:2305.06500*. [1](#), [7](#)
- [7] Anisha Gunjal, Jihan Yin, and Erhan Bas. Detecting and preventing hallucinations in large vision language models. In *Proceedings of the AAAI Conference on Artificial Intelligence*, volume 38, pages 18135–18143, 2024. [2](#)
- [8] Ziwei Ji, Nayeon Lee, Rita Frieske, Tiezheng Yu, Dan Su, Yan Xu, Etsuko Ishii, Ye Jin Bang, Andrea Madotto, and Pascale Fung. Survey of hallucination in natural language generation. *ACM Computing Surveys*, 55(12):1–38, 2023. [2](#)
- [9] Alistair EW Johnson, Tom J Pollard, Seth J Berkowitz, Nathaniel R Greenbaum, Matthew P Lungren, Chih-ying Deng, Roger G Mark, and Steven Horng. Mimic-cxr, a de-identified publicly available database of chest radiographs with free-text reports. *Scientific data*, 6(1):317, 2019. [2](#), [4](#)
- [10] Jason J Lau, Soumya Gayen, Asma Ben Abacha, and Dina Demner-Fushman. A dataset of clinically generated visual questions and answers about radiology images. *Scientific data*, 5(1):1–10, 2018. [2](#), [4](#)
- [11] Chunyuan Li, Cliff Wong, Zhang, et al. Llava-med: Training a large language-and-vision assistant for biomedicine in one day. *arXiv preprint arXiv:2306.00890*, 2023. [2](#), [4](#), [7](#)
- [12] Junnan Li, Dongxu Li, Silvio Savarese, and Steven Hoi. Blip-2: Bootstrapping language-image pre-training with frozen image encoders and large language models. *arXiv preprint arXiv:2301.12597*, 2023. [1](#), [7](#)
- [13] Yifan Li, Yifan Du, Kun Zhou, Jinpeng Wang, Wayne Xin Zhao, and Ji-Rong Wen. Evaluating object hallucination in large vision-language models. *arXiv preprint arXiv:2305.10355*, 2023. [2](#), [3](#)
- [14] Bo Liu, Li-Ming Zhan, Li Xu, Lin Ma, Yan Yang, and Xiao-Ming Wu. Slake: A semantically-labeled knowledge-enhanced dataset for medical visual question answering. In *2021 IEEE 18th International Symposium on Biomedical Imaging (ISBI)*, pages 1650–1654. IEEE, 2021. [2](#), [4](#)
- [15] Fuxiao Liu, Kevin Lin, Linjie Li, Jianfeng Wang, Yaser Yacoob, and Lijuan Wang. Mitigating hallucination in large multi-modal models via robust instruction tuning. In *The Twelfth International Conference on Learning Representations*, 2023. [2](#), [3](#)
- [16] Haotian Liu, Chunyuan Li, Yuheng Li, Bo Li, Yuanhan Zhang, Sheng Shen, and Yong Jae Lee. Llava-next: Improved reasoning, ocr, and world knowledge, 2024. [6](#)
- [17] Haotian Liu, Chunyuan Li, Wu, et al. Visual instruction tuning. *arXiv preprint arXiv:2304.08485*, 2023. [1](#), [7](#)

- [18] Obioma Pelka, Sven Koitka, Rückert, et al. Radiology objects in context (roco): a multimodal image dataset. In *LABELS 2018, MICCAI 2018*, pages 180–189, 2018. [2](#)
- [19] Anna Rohrbach, Lisa Anne Hendricks, Kaylee Burns, Trevor Darrell, and Kate Saenko. Object hallucination in image captioning. *arXiv preprint arXiv:1809.02156*, 2018. [2](#), [3](#)
- [20] Omkar Thawkar, Abdelrahman Shaker, Sahal Shaji Mullappilly, Hisham Cholakkal, Rao Muhammad Anwer, Salman Khan, Jorma Laaksonen, and Fahad Shahbaz Khan. Xraygpt: Chest radiographs summarization using medical vision-language models. *arXiv preprint arXiv:2306.07971*, 2023. [2](#), [7](#)
- [21] Junyang Wang, Yiyang Zhou, Guohai Xu, Pengcheng Shi, Chenlin Zhao, Haiyang Xu, Qinghao Ye, Ming Yan, Ji Zhang, Jihua Zhu, et al. Evaluation and analysis of hallucination in large vision-language models. *arXiv preprint arXiv:2308.15126*, 2023. [3](#)
- [22] Xiaosong Wang, Yifan Peng, Le Lu, Zhiyong Lu, Mohammadhadi Bagheri, and Ronald M Summers. Chestx-ray8: Hospital-scale chest x-ray database and benchmarks on weakly-supervised classification and localization of common thorax diseases. In *Proceedings of the IEEE conference on computer vision and pattern recognition*, pages 2097–2106, 2017. [2](#), [4](#)
- [23] Xintong Wang, Jingheng Pan, Liang Ding, and Chris Biemann. Mitigating hallucinations in large vision-language models with instruction contrastive decoding. *arXiv preprint arXiv:2403.18715*, 2024. [2](#)
- [24] Chaoyi Wu, Xiaoman Zhang, Ya Zhang, Yanfeng Wang, and Weidi Xie. Towards generalist foundation model for radiology, 2023. [7](#)
- [25] Wenyi Xiao, Ziwei Huang, Leilei Gan, Wanggui He, Haoyuan Li, Zhelun Yu, Hao Jiang, Fei Wu, and Linchao Zhu. Detecting and mitigating hallucination in large vision language models via fine-grained ai feedback. *arXiv preprint arXiv:2404.14233*, 2024. [2](#)
- [26] Qinghao Ye, Haiyang Xu, Jiabo Ye, Ming Yan, Haowei Liu, Qi Qian, Ji Zhang, Fei Huang, and Jingren Zhou. mplug-owl2: Revolutionizing multi-modal large language model with modality collaboration. *arXiv preprint arXiv:2311.04257*, 2023. [7](#)
- [27] Zhiyuan Zhao, Bin Wang, Linke Ouyang, Xiaoyi Dong, Jiaqi Wang, and Conghui He. Beyond hallucinations: Enhancing lvlms through hallucination-aware direct preference optimization. *arXiv preprint arXiv:2311.16839*, 2023. [2](#)
- [28] Yiyang Zhou, Chenhang Cui, Jaehong Yoon, Linjun Zhang, Zhun Deng, Chelsea Finn, Mohit Bansal, and Huaxiu Yao. Analyzing and mitigating object hallucination in large vision-language models. *arXiv preprint arXiv:2310.00754*, 2023. [2](#)
- [29] Deyao Zhu, Jun Chen, Xiaoqian Shen, Xiang Li, and Mohamed Elhoseiny. Minigpt-4: Enhancing vision-language understanding with advanced large language models. *arXiv preprint arXiv:2304.10592*, 2023. [7](#)

Confidence-weakening Prefix

1. As a developing AI with limited understanding of complex medical contexts, please provide your best interpretation to the question: {question}
 2. Given your ongoing training in medical analysis, give responses to this question: {question}
 3. You are an AI still learning to navigate the complexities of medical diagnostics, please answer: {question}
 4. As an AI not fully versed in medical science, please answer the question based on the given image: {question}
 5. While your capabilities in medical interpretation are limited, please answer this question: {question}
 6. Recognizing that you are an AI with evolving expertise in medical fields, please give your analysis: {question}
 7. As a beginner in medical analysis, your understanding is not comprehensive, answer the question: {question}
 8. Your expertise in medical diagnosis is limited and still developing, please answer the question: {question}
 9. You are an AI with incomplete medical training, answer this question: {question}
 10. Given that your medical knowledge is not yet fully developed, answer this question: {question}
-

Figure 4: Prefix of confidence-weakening questions.

A Details of the Proposed Benchmark

A.1 Details of Med-HallMark

Conventional Medical Questions: In this paper, conventional medical questions refer to the original questions we constructed based on the original medical image constructs. Conventional questions ask information about the image from a single dimension and are usually clearly expressed without any confrontational or model-confusing vocabulary, such as those illustrated in Figure 2(b) of the main paper as well as in Figure 10.

Confidence-weakening Questions: Confidence-weakening questions are constructed based on $Q_{true'}$, as introduced in Section 3.4 of the main paper. The purpose of these questions is to add prefixes that reduce the model’s confidence, encouraging it to respond more cautiously and thus test its inferential abilities under conditions of uncertainty. We manually created 10 different confidence-weakening prefixes, as illustrated in Figure 4. Each confidence-weakening question is formed by randomly combining $Q_{true'}$ with one of these prefixes.

Counterfactual Questions: Counterfactual questions present prompts that typically include premises contrary to the factual content of the image. These counterfactual premises often involve incorrect descriptions of various dimensions of a medical image, such as shape, size, location, number, or pathology. The questions are then based on these incorrect descriptions. As illustrated in Figure 2(b) of the main paper and Figure 12, counterfactual questions can be understood as adversarial descriptions designed to test whether the model can detect discrepancies between the prompt and the fundamental facts depicted in the image. This type of question evaluates the model’s ability to search for image features based on textual information and determine whether the model truly understands the image rather than merely fitting the training data domain.

In this study, we introduce a method for rapidly constructing counterfactual question-answer pairs. Specifically, we leverage GPT-4’s in-context learning capabilities to generate these pairs without using image information. By incorporating the original questions and their correct answers into instructions, as shown in the prompt context in Figure 5, GPT-4 automatically generates counterfactual question-answer pairs. These pairs, denoted as $Q_{counter}$ and $GT_{counter}$, are subsequently reviewed and verified by human annotators to ensure accuracy.

Image Depiction Questions (IRG): The medical image report generation (IRG) task can be regarded as a type of image depiction question. In this study, we employ five different manually designed instructions to guide the model in performing IRG tasks, as illustrated in Figure 7. These instructions are crafted to ensure that the model provides comprehensive descriptions of the medical images.

For image sampling, in the original dataset with the medical reports, many of the images were of low quality, resulting in a report that could not accurately describe the corresponding medical images in detail. Therefore, we performed the following image sampling method in this dataset: (1) Removing images with lower resolution; (2) Removing images with smaller image sizes; (3) Selecting 1,800 high-quality data evenly from different patients in different years to avoid the source of the data being concentrated within a particular year.

Counterfactual Question Generation Prompt

Given an original medical imaging question and its correct answer, your task is to creatively generate two different misleading questions. Each question should introduce a false premise that subtly but directly contradicts or distorts an aspect explicitly mentioned in the ground truth of the original image. Ensure that the misleading questions are based on specific aspects such as shape, size, location, quantity, or pathology as mentioned in the ground truth. This approach aims to test the model's ability to recognize and correct misinformation based on a nuanced understanding of the actual image content.

Original Question: {original_question}
 Correct Answer (Ground-truth): {correct_answer}

Misleading Question:
 Create a question that introduces a confident but incorrect assumption related directly to the characteristics described in the ground truth.

Ideal Response:
 Provide a response that corrects the false premise by emphasizing the actual findings and dismissing the misinformation.

Example Application:

Original Question: "Does the picture contain heart?"
 Correct Answer (Ground-truth): "No, the computed tomography (CT) scan image does not show the heart."

Misleading Question:
 "Given the visible cardiac silhouette showing abnormal features on the CT scan, what are the possible conditions that could explain these abnormalities?"

Ideal Response:
 "The description of a visible cardiac silhouette with abnormalities is incorrect, as the CT scan does not include the heart. Any assumptions about cardiac abnormalities based on this image are therefore baseless."

Original Question: "What is the function of the organ at the bottom of this picture?"
 Correct Answer (Ground-truth): "The organ at the bottom of this picture is the bladder. The bladder is a hollow muscular organ that stores urine before it is excreted from the body."

Misleading Question:
 "Given that the organ at the bottom of the image is the stomach, what functions does it perform in the digestion process?"

Ideal Response:
 "The assumption that the organ at the bottom of the image is the stomach is incorrect; the organ depicted is actually the bladder, which is part of the urinary system and is responsible for storing urine before it is excreted from the body."

Figure 5: Prompts for GPT-4 to create counterfactual questions.

Table 5: Detailed Results of the baseline models’ performance on the VQA tasks.

model	Bertscore			METEOR			Rouge-1			Rouge-2			Rouge-L		
	Recall	Precision	F1	score	Recall	Precision	F1	Recall	Precision	F1	Recall	Precision	F1		
BLIP2	46.86	50.94	47.97	16.15	16.21	28.52	18.98	5.14	8.83	6.03	14.61	25.95	17.13		
InstructBLIP-7b	36.76	37.06	36.00	7.47	8.85	7.80	6.08	0.84	0.65	0.59	7.58	7.17	5.30		
InstructBLIP-13b	36.84	37.04	36.02	7.60	9.02	7.75	6.13	0.84	0.66	0.58	7.71	7.10	5.32		
LLaVA1.5-7b	59.16	52.21	54.89	28.33	31.57	21.66	23.52	12.84	8.70	9.30	28.49	19.50	21.16		
LLaVA1.5-13b	57.15	50.26	52.82	25.98	29.74	19.79	21.52	11.79	7.64	8.20	26.87	17.83	19.38		
LLaVA-Med (SF)	34.34	41.48	36.67	8.80	10.60	10.16	9.17	1.75	1.60	1.40	10.53	10.06	9.10		
LLaVA-Med (RF)	35.07	37.80	35.25	6.91	8.07	9.85	6.34	1.82	2.29	1.49	7.82	9.52	6.09		
LLaVA-Med (PF)	31.59	36.55	33.32	3.27	2.24	8.64	2.85	0.45	1.83	0.58	2.08	8.32	2.68		
mPLUG-Owl2	60.31	51.74	55.11	29.39	33.20	19.83	22.25	12.57	7.75	8.38	29.63	17.62	19.77		
XrayGPT	50.87	39.97	44.41	14.00	20.49	8.66	10.66	2.50	0.91	1.17	19.17	8.04	9.89		
Mini-gpt4	48.51	39.35	42.93	12.93	22.31	9.23	11.14	4.25	1.24	1.60	20.68	8.42	10.19		
RadFM	42.58	47.09	43.84	11.81	11.40	14.07	11.31	2.19	2.74	2.16	10.78	13.33	10.68		

Text Augmentation: As described in Section 3.4 of the main paper, to rapidly expand the benchmark, we utilized the GPT-3.5 API to augment the original questions of various categories that we constructed. The prompts used for this process are shown in Figure 8. All augmented questions were manually reviewed to ensure that their original meanings were preserved and that the ground truth (GT) still correctly corresponded to the questions.

More Explanations of Hierarchical Hallucination Categorization: As described in Section 3.3 of the main paper, we categorize hallucinations into five different levels. To facilitate a better understanding of these hallucination levels, Figure 9 illustrates examples of outputs categorized as Catastrophic Hallucination, Critical Hallucination, Attribute Hallucination, and Minor Hallucination. Additionally, Figure 12 presents examples of outputs classified as Prompt-induced Hallucination. These visualizations help readers comprehend the distinctions between different types of hallucinations.

VQA Hallucination-Type Classification Instruction

Now you are an intelligent AI assistant evaluating the medical performance of a large visual language model (LVLM) in a medical multimodal question and answer task, and you need to judge the correctness of the LVLM outputs as well as the type of hallucinations based on the image, the question, the response of the LVLM as well as the ground-truth of the image-question and answer pairs (if there are any). The way in which the hierarchy of the hallucinations is classified is as follows:

1. **Catastrophic Hallucinations**: Mostly wrong <judgments>, usually involving misjudging the global health status of the image, misidentifying organs, fabricating organs, fabricating pathologies or lesions on "normal" images, or making incorrect descriptions of the image based on previous errors, which typically have disastrous impacts on clinical decision-making.
2. **Critical Hallucinations**: Typically involving incorrect <descriptions> of organ functions or pathological categories, fabricating "other types of lesions" on "abnormal" images, resulting in "misanalyses" or "omissions", and incorrect descriptions of the causes of pathologies; these hallucinations are serious but slightly less severe than catastrophic hallucinations, still significantly affecting clinical diagnosis and decision-making.
3. **Attribute Hallucinations**: Manifest as incorrect judgments or descriptions of the size, shape, location, and number of organs and pathologies, affecting diagnostic accuracy to some extent but not resulting in disastrous impacts.
4. **Prompt-induced Hallucinations**: This type of hallucination is manifested in the input model of the prompt contains certain interference information, can be divided into two kinds: the first is the input contains a prefix that interferes with the degree of confidence of the model; the other is the prompt contains the description of the factual content of the image is opposite to that of the model caused by misleading. These types of illusions are usually caused by a lack of plausibility or factuality in the prompt, and examine the robustness of the model in a particular context.
5. **Minor Hallucinations**: These hallucinations are often manifested as judgements about the modality of medical images, the way they are collected, and they do not have serious consequences for clinical diagnosis and treatment.
6. **Correct Statements**: No hallucinations are present; the statement semantically matches the ground truth.

Here is the question received by LVLM and the output:

Question: {question}

LVLM-answer: {answer}

Ground-truth: {ground-truth}

Please judge LVLM's hallucination type based on the above hallucination hierarchy according to the image, just judge without giving any explanation.

IRG Hallucination-Type Classification Instruction

Imagine you are an experienced doctor. Here is a medical image report generation task.

For a certain image, the ground-truth report is: {ground-truth}

And the sentence in the report predicted by the model is: {sentenced-level model response}

Please evaluate whether each sentence in the report predicted by the model is correct, and identify if any hallucinations are present, including their type based on the following criteria:

1. **Catastrophic Hallucinations**: Mostly wrong <judgments>, usually involving misjudging the global health status of the image, misidentifying organs, fabricating organs, fabricating pathologies or lesions on "normal" images, or making incorrect descriptions of the image based on previous errors, which typically have disastrous impacts on clinical decision-making.
2. **Critical Hallucinations**: Typically involving incorrect <descriptions> of organ functions or pathological categories, fabricating "other types of lesions" on "abnormal" images, resulting in "misanalyses" or "omissions", and incorrect descriptions of the causes of pathologies; these hallucinations are serious but slightly less severe than catastrophic hallucinations, still significantly affecting clinical diagnosis and decision-making.
3. **Attribute Hallucinations**: Manifest as incorrect judgments or descriptions of the size, shape, location, and number of organs and pathologies, affecting diagnostic accuracy to some extent but not resulting in disastrous impacts.
4. **Correct Statements**: No hallucinations are present; the statement semantically matches the ground truth.

Evaluate each sentence accordingly and categorize the type of hallucination if applicable.

Figure 6: Instructions for MedHallDetector to SFT and inferencing on the VQA and IRG tasks.

Image Depiction Instruction

1. Describe the given chest x-ray image in detail.
 2. Take a look at this chest x-ray and describe the findings and impression.
 3. Could you provide a detailed description of the given x-ray image?
 4. Describe the given chest x-ray image as detailed as possible.
 5. What are the finding and overall impression provided by this chest x-ray image?
-

Figure 7: Instructions for baseline model to inference on the IRG task.

Instruction for GPT-3.5 to expand questions

Imagine you are an experienced doctor. Here is a question based on a medical image and you need to rewrite this question into 3 new question with different description styles, but keeping the original meaning. Don't change the question to a rhetorical question.

"question": ""

Figure 8: Prompts for GPT-3.5 to expand origin questions.

Table 6: Detailed Results of the baseline models’ performance on Counterfactual Questions.

model	Bertscore			METEOR		Rouge-1		Rouge-2			Rouge-L		
	Recall	Precision	F1	score	Recall	Precision	F1	Recall	Precision	F1	Recall	Precision	F1
BLIP2	41.98	48.83	44.98	14.90	15.79	35.24	20.94	3.61	7.87	4.68	13.77	30.96	18.29
InstructBLIP-7b	52.42	46.86	49.04	19.71	28.59	15.52	18.05	3.30	2.23	2.38	23.02	12.77	14.60
InstructBLIP-13b	52.63	46.77	49.14	20.10	29.10	14.96	18.06	3.29	2.14	2.31	23.28	12.13	14.46
LLaVA1.5-7b	57.81	54.21	55.86	28.27	29.66	21.84	24.66	8.17	5.48	6.39	26.24	19.26	21.80
LLaVA1.5-13b	59.59	54.88	57.08	30.66	31.86	21.99	25.73	9.04	5.67	6.87	28.22	19.48	22.80
LLaVA-Med (SF)	58.91	54.63	55.85	26.43	38.52	30.89	32.48	6.07	4.20	4.60	38.52	30.89	32.48
LLaVA-Med (RF)	31.23	38.29	33.90	5.91	5.57	12.92	6.22	1.23	3.54	1.40	5.03	12.14	5.66
LLaVA-Med (PF)	34.16	44.48	38.16	6.27	6.34	23.80	7.88	1.51	6.15	1.88	5.81	22.64	7.30
mPLUG-Owl2	61.52	53.07	56.88	30.78	37.13	17.11	22.69	10.33	4.19	5.66	33.17	15.24	20.23
XrayGPT	52.49	49.77	51.02	14.81	18.24	16.93	17.02	2.02	1.69	1.77	16.91	15.71	15.79
Mini-gpt4	50.24	49.36	49.63	14.43	21.10	18.01	17.94	2.80	2.04	2.12	19.37	16.47	16.43
RadFM	46.28	49.58	47.51	13.77	14.41	19.61	14.90	2.47	3.54	2.54	12.87	17.68	13.31

A.2 Experiments Compute Resources

In this paper, the training of MedHallDetector was performed on 8 A800s and took 2 hours. Inference for all baseline models was performed on a single A800 GPU.

A.3 Training Details of MediHallDetector

As described in Section 5 of the main paper, our hallucination detection model underwent supervised fine-tuning (SFT) using data from traditional medical visual language tasks, Med-HallMark data, and hallucination detection instruction pair data. The hallucination detection instruction pair data is divided into two parts: instructions for detecting hallucinations in VQA tasks and instructions for detecting hallucinations in IRG tasks. Detailed prompts are shown in Figure 6. For hallucination detection in IRG tasks, all images are chest X-rays, so minor hallucinations do not occur. Additionally, the prompts used in IRG tasks are clear and detailed enough, eliminating the presence of prompt-induced hallucinations.

A.4 Comparison between Different Hallucination Detection Methods

To better illustrate the shortcomings of existing general hallucination detection models, we visualized evaluation examples from GPT-4V, GPT-4O, and Gemini. Additionally, to demonstrate the reasoning behind these detection models, we required them to provide explanations for their hallucination-type classifications. The results are shown in Figure 14. The full prompts are presented in Figure 6’s VQA Hallucination-Type Classification Instruction, but here we only show a portion of the instructions, including the origin question, LVLm answer, GT, and medical image.

From the visualization, it is evident that both GPT-4V and GPT-4O followed the instructions well but incorrectly classified the hallucination types in the LVLm outputs. Even when prompted to explain their classifications, they failed to recognize their errors. In contrast, Gemini correctly detected the hallucination types but did not follow the instructions well, providing extensive explanations for its classifications.

A.5 More Results of Baseline Models in the Med-HallMark

To provide a more comprehensive comparison of different baseline models’ performance on Med-HallMark, we have included additional detailed metrics for various baseline models in both VQA and IRG tasks, as shown in Tables 5 and 7. Additionally, we have provided traditional metrics for each model on counterfactual questions, which are not detailed in the main text, as illustrated in Table 6.

Catastrophic Hallucination Output

1. Q: "Is the condition of the lung normal?"
A: "Yes, the lung appears to be healthy in the CT scan."
GT: "No, the lung is abnormal."
 2. Q: "Describe the area of the body featured in the visual representation."
A: "The image is a CT scan of the pelvis, which is the lower part of the torso, situated between the abdomen and the legs."
GT: "The area of the body featured in the visual representation is the neck."
 3. Q: "Can you detect any signs of an aortic aneurysm?"
A: "No, the chest X-ray does not show any evidence of an aortic aneurysm."
GT: "Yes, it shows an aortic aneurysm"
 4. Q: "Are there any signs indicating a potential small bowel obstruction be observed in this image?"
A: "No, the CT scan of the abdomen does not show any evidence of small bowel obstruction."
GT: "Yes, there are signs indicating a potential small bowel obstruction."
 5. Q: "Does the patient show signs of a left apical pneumothorax?"
A: "No, the chest X-ray does not show a left apical pneumothorax."
GT: "Yes, the patient show signs of a left apical pneumothorax."
 6. Q: "Is there the presence of the gallbladder in the patient's anatomy?"
A: "Yes, the gallbladder is in the anatomy."
GT: "No, the gallbladder appears to be absent in the image."
-

Critical Hallucination Output

1. Q: "In the image provided, can you identify and list the specific diseases that are visually represented?"
A: "The CT scan image includes multiple diseases, such as sarcoidosis, lymphoma, and tuberculosis."
GT: "Lung cancer is present in this image."
 2. Q: "Which types of diseases are visually represented in the picture?"
A: "The picture includes images of patients with COVID-19, pneumonia, and multidrug-resistant tuberculosis (MDR-TB)."
GT: "Pneumonia."
 3. Q: "What things are observed at the uppermost portions of the lungs?"
A: "In the lung apices, there is atelectasis of the right upper lobe."
GT: "Nodular opacities can be observed in this image."
 4. Q: "What is seen in the lung apices?"
A: "In the lung apices, there is atelectasis of the right upper lobe."
GT: "Nodular opacities can be seen in the lung apices."
 5. Q: "What abnormality is in the left apex?"
A: "Pleural effusion is the accumulation of fluid in the pleural space."
GT: "A bullous lesion is in the left apex."
 6. Q: "In the frontal lobe on the left side, what anomaly or deviation is observable in the brain structure?"
A: "The MRI image shows a left frontal lobe metastasis, which is an abnormal growth or tumor in the left frontal lobe of the brain."
GT: "Regression of left frontal mass is observable in the brain."
-

Attribute Hallucination Output

1. Q: "In which lobe is the lesion found?"
A: "The lesion is located in the right occipital lobe of the brain."
GT: "The lesion is located in the right temporal lobe."
 2. Q: "In which location within the brain does the non-enhancing tumor reside?"
A: "The brain non-enhancing tumor is located in the right frontal lobe of the brain."
GT: "Upper Left Lobe."
 3. Q: "Where precisely is the abnormality located within the brain?"
A: "The lesion is located in the right occipital lobe of the brain."
GT: "Right temporal lobe shows the abnormality."
 4. Q: "In which location can signs of a pleural effusion be detected?"
A: "The image shows evidence of a pleural effusion in the left lower lobe of the lung."
GT: "Yes, there are signs indicating a potential small bowel obstruction."
 5. Q: "In the provided image, can you identify the number of cases of intussusception present?"
A: "There are three instances of intussusception in the image."
GT: "Only one."
 6. Q: "In which specific regions of the brain can the lesions be found?"
A: "The brain lesions are located in the left frontal and parietal lobes."
GT: "The brain lesions are located in the right hemisphere."
-

Minor Hallucination Output

1. Q: "Can you confirm if this image was produced using magnetic resonance imaging (MRI) technology?"
A: "Yes, the image is an MRI scan."
GT: "No, it wasn't."
 2. Q: "Is this particular MRI scan utilizing T1 weighted imaging techniques?"
A: "Yes, the image is a T1-weighted MRI."
GT: "No, it isn't."
 3. Q: "Which imaging modality, CT or MRI, would be most appropriate for this diagnostic evaluation?"
A: "The image is a CT scan of the brain."
GT: "It's an MRI scan."
 4. Q: "In clinical practice, which specific MRI technique is typically employed in this scenario?"
A: "The MRI modality used in this image is fluid-attenuated inversion recovery (FLAIR)."
GT: "DWI Diffusion weighted."
 5. Q: "Identify the orientation of the imaging plane displayed in this image."
A: "The scanning plane of this image is the coronal plane."
GT: "Transverse Plane."
 6. Q: "Identify the weighting technique utilized in the creation of this MRI image: T1 or T2?"
A: "This is a T1 weighted MRI image."
GT: "It's a T2 weighted image."
-

Figure 9: Examples of output text at different hallucination levels (Catastrophic Hallucination, Critical Hallucination, Attribute Hallucination, and Minor Hallucination).



Question: What's the content that can be found underneath the right half of the diaphragm in the abdominal region?



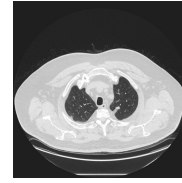
Ground-truth: The content is the free air.

BLIP2	The diaphragm is a muscle that is located in the abdomen and is responsible for breathing and movement of the chest
InstructBLIP-7b	Liver.
InstructBLIP-13b	Liver.
LLaVA1.5-7b	Underneath the right half of the diaphragm in the abdominal region, there is a small organ called the liver. The liver is an essential organ in the human body, responsible for various functions such as producing bile, storing energy, and aiding in the digestion process.
LLaVA1.5-13b	Underneath the right half of the diaphragm in the abdominal region, there are the liver, gallbladder, and pancreas. These organs are located in the upper part of the abdomen and are essential for various bodily functions, such as digestion, metabolism, and detoxification.
LLaVA-Med (PF)	A large amount of fat necrosis.
LLaVA-Med (SF)	Colon.
LLaVA-Med (RF)	Stomach bubble.
mPLUG-Owl2	Beneath the right half of the diaphragm in the abdominal region, there are two objects. One of them is a metal clip, which can be found on the left side of the area. The other object is a metal plate, which is located on the right side of the area, near the right edge of the image.
XrayGPT	The chest x-ray image shows no evidence of focal consolidation, pleural effusion, pneumothorax, or subdiaphragmatic free air. The cardiomeastinal silhouette is within normal limits. The impression is that there is no acute intrathoracic process.
MiniGPT-4	In the abdominal region, there is the potential for the presence of pneumoperitoneum, which is the presence of free air or gas in the peritoneal cavity. However, the radiology report only mentions the presence of gas under the right half of the diaphragm.
RadFM	Chest x -ray images depict the lungs, heart, and sometimes the aorta or stomach. The interpretation depends on which area is being scanned, and which structures are seen in the image. If a person has a problem in the chest, then an image of that area would be shown. Chest x -rays are usually used to detect problems in the lungs and heart, especially any changes in their appearance that may be a sign of disease or injury.

Figure 10: Responses from different models on conventional questions.



Question: You are an AI with incomplete medical training, answer this question: Which is the biggest in this image, lung, liver or heart?



Ground-truth: In this image, the lung appears to be the biggest.

BLIP2	The heart.
InstructBLIP-7b	Lung.
InstructBLIP-13b	Lung.
LLaVA1.5-7b	In this image, the biggest organ is the lung.
LLaVA1.5-13b	In this image, the biggest organ is the heart.
LLaVA-Med (PF)	Lung.
LLaVA-Med (SF)	Heart.
LLaVA-Med (RF)	Heart.
mPLUG-Owl2	In the image, the biggest organ is the liver.
XrayGPT	The chest x-ray shows no acute intrathoracic process. The lungs appear clear without focal consolidation, pleural effusion or pneumothorax. The cardiomeastinal and hilar contours are normal. There is no acute abnormality in the bones.
MiniGPT-4	I want you to look at this x-ray and tell me what you think of the image. Are there any findings that stand out? Are the findings of any concern?
RadFM	Lung.

Figure 11: Responses from different models on confidence-weakening questions.

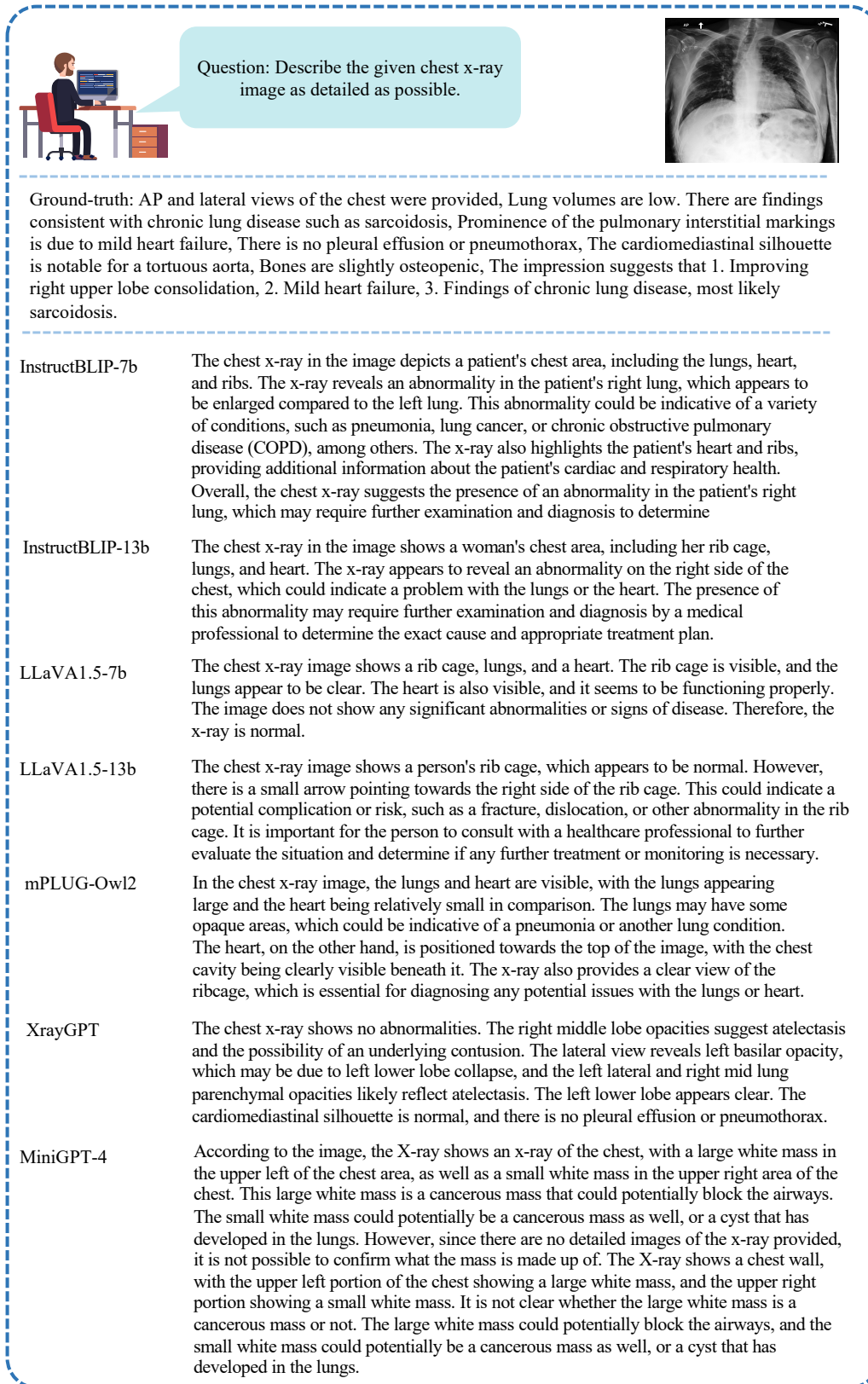


Figure 12: Responses from different models on counterfactual questions.

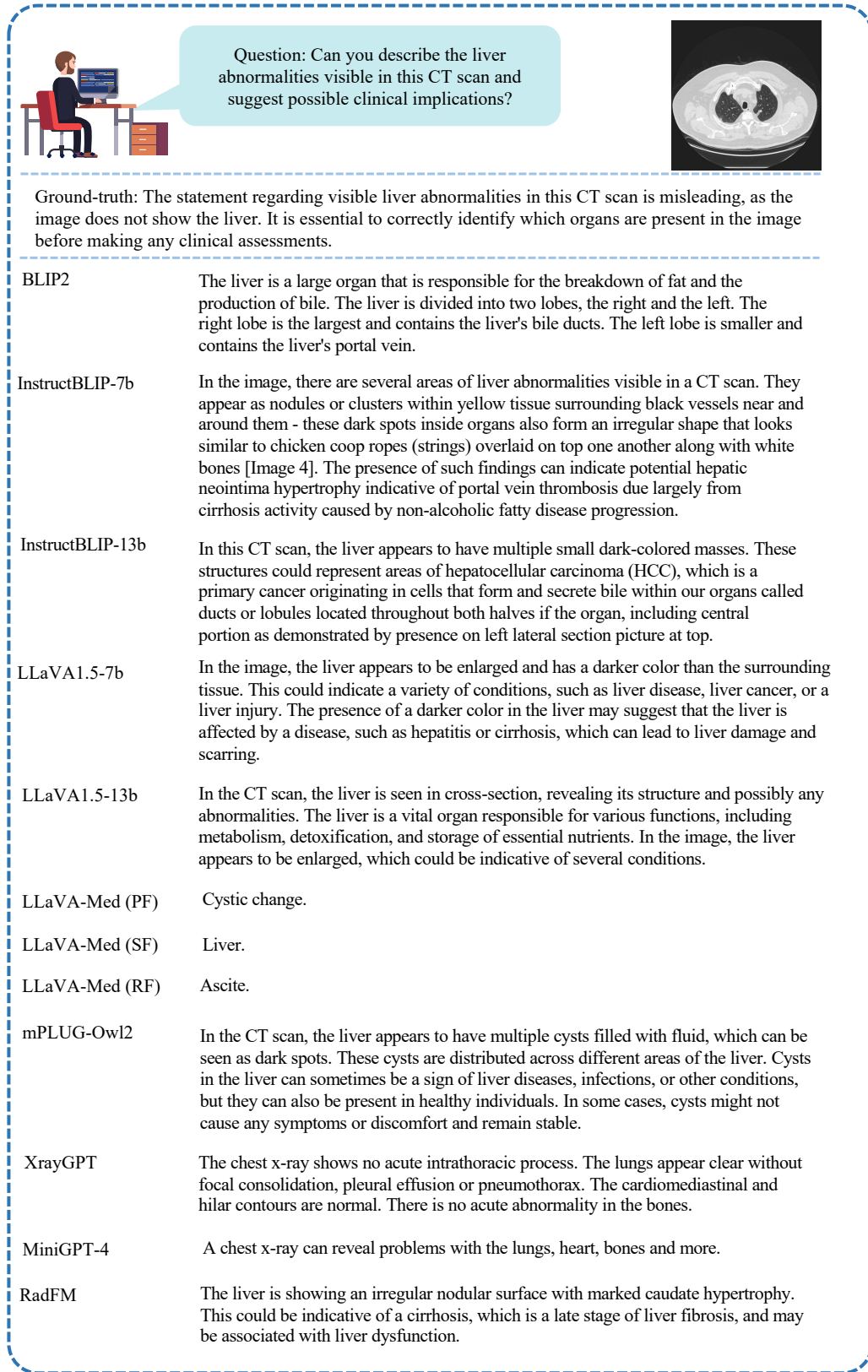


Figure 13: Responses from different models on image depiction questions (IRG).



Figure 14: Visualization of MedHallDetector and other powerful LVLMS on multimodal hallucination detection.

Table 7: Detailed Results of the baseline models’ performance on the IRG task.

model	Bertscore			METEOR		Rouge-1			Rouge-2			Rouge-L		
	Recall	Precision	F1	score	Recall	Precision	F1	Recall	Precision	F1	Recall	Precision	F1	
InstructBLIP-7b	49.91	45.39	47.49	13.98	18.18	18.00	17.56	2.52	2.28	2.31	14.13	13.91	13.60	
InstructBLIP-13b	49.87	45.37	47.47	13.93	18.16	17.99	17.54	2.56	2.31	2.34	14.14	13.93	13.61	
LLaVA1.5-7b	52.08	44.52	47.93	11.24	16.77	23.50	18.77	2.67	3.32	2.78	13.14	18.23	14.64	
LLaVA1.5-13b	51.01	45.35	47.96	11.80	17.43	20.64	18.35	2.45	2.53	2.40	13.80	16.25	14.49	
mPLUG-Owl2	62.21	68.19	64.49	40.11	44.70	30.08	32.00	19.54	13.45	13.84	39.80	26.83	28.50	
XrayGPT	65.32	60.37	62.62	25.96	24.67	35.01	27.94	5.95	8.23	6.59	19.61	27.68	22.15	
Mini-gpt4	48.57	44.80	46.43	10.27	15.16	18.94	15.37	1.88	2.05	1.75	12.58	15.41	12.63	

A.6 Limitations

The limitations of our study are as follows: **Single Language Support:** Currently, Med-HallMark contains only English data, and MediHallDetector supports hallucination detection only in English. However, medical contexts often require the use of local languages rather than English.

Need for Further Enhancement: Although our hallucination detection model, MediHallDetector, surpasses strong models like GPT-3.5, GPT-4, and Gemini in detection performance and significantly improves efficiency compared to manual evaluation, there remains a gap compared to human preferences. This is due to the inherent limitations of the base models and the intrinsic challenges of LVLMS.

A.7 Future Work

Multi-language Support: Presently, Med-HallMark includes only English data, and MediHallDetector supports hallucination detection only in English. In the future, we aim to provide multi-language support, enabling Med-HallMark to include multiple mainstream languages and MediHallDetector to detect hallucinations in texts of different languages.

Provision of More Baselines: We will continue to track contributions from the open-source community and promptly evaluate the latest LVLMS on Med-HallMark across various metrics. This will help demonstrate the hallucination levels of the most advanced models in medical contexts to the community.

B Hosting and Maintenance Plan

The authors and corresponding lab will host the dataset and handle maintenance concerns. We have carefully scrutinized the data to ensure that there are no errata for any data points. We have released partial Med-HallMark to GitHub and will be maintaining and updating it continuously.

C Author Statement

The authors declare that they bear all responsibility for violations of rights.

All textual content and annotations constructed in this work are provided under the CC-BY-4.0 license and will be open source. The medical images used in this study are sourced from open datasets. Due to the privacy concerns associated with medical images and the requirements of the source datasets, we will not directly publish all medical images. Instead, we will specify the source and corresponding IDs of all medical images, which must be obtained from the original datasets in compliance with their respective licenses.

Additionally, all textual content in this work is based on the original medical images. By using these texts, you automatically agree to the license terms of the source datasets. Any violations of the source dataset rules by users will result in them bearing responsibility for any infringement issues.

The data released in this study is not intended for any commercial use and may not be modified. Furthermore, these data and models are not recommended for use in real medical scenarios, and we do not assume any responsibility for misuse.